

Article

Deep Learning Framework for Accurate Static and Dynamic Prediction of CO₂ Enhanced Oil Recovery and Storage Capacity

Zhipeng Xiao ¹, Bin Shen ^{2,*} , Jiguang Yang ¹, Kun Yang ², Yanbin Zhang ¹ and Shenglai Yang ^{2,*}

¹ Exploration and Development Research Institute, PetroChina Tuha Oil & Gasfield Company, Xinjiang 839009, China; xiaozp_th@163.com (Z.X.); yjg_th@163.com (J.Y.); yanbinzhang_th@163.com (Y.Z.)

² National Key Laboratory of Petroleum Resources and Engineering, China University of Petroleum (Beijing), Beijing 102249, China; yangkun_cup@163.com

* Correspondence: binshen0803@163.com (B.S.); yangsl@cup.edu.cn (S.Y.)

Abstract: As global warming intensifies, carbon capture, utilization, and storage (CCUS) technology is widely used to reduce greenhouse gas emissions. CO₂-enhanced oil recovery (CO₂-EOR) technology has, once again, received attention, which can achieve the dual benefits of oil recovery and CO₂ storage. However, flexibly and effectively predicting the CO₂ flooding and storage capacity of potential reservoirs is a major problem. Traditional prediction methods often lack the ability to comprehensively integrate static and dynamic predictions and, thus, cannot fully understand CO₂-EOR and storage capacity. This study proposes a comprehensive deep learning framework, named LightTrans, based on a lightweight gradient boosting machine (LightGBM) and Temporal Fusion Transformers, for dynamic and static prediction of CO₂-EOR and storage capacity. The model predicts cumulative oil production, CO₂ storage amount, and Net Present Value on a test set with an average R-square (R²) of 0.9482 and an average mean absolute percentage error (MAPE) of 0.0143. It shows great static prediction performance. In addition, its average R² of dynamic prediction is 0.9998, and MAPE is 0.0025. It shows excellent dynamic prediction ability. The proposed model successfully captures the time-varying characteristics of CO₂-EOR and storage systems. It is worth noting that our model is 10⁵–10⁶ times faster than traditional numerical simulators, which once again demonstrates the high-efficiency value of the LightTrans model. Our framework provides an efficient, reliable, and intelligent solution for the development and optimization of CO₂ flooding and storage.



Citation: Xiao, Z.; Shen, B.; Yang, J.; Yang, K.; Zhang, Y.; Yang, S. Deep Learning Framework for Accurate Static and Dynamic Prediction of CO₂ Enhanced Oil Recovery and Storage Capacity. *Processes* **2024**, *12*, 1693. <https://doi.org/10.3390/pr12081693>

Academic Editor: Jorge Ancheytá

Received: 28 June 2024

Revised: 8 August 2024

Accepted: 11 August 2024

Published: 13 August 2024



Copyright: © 2024 by the authors. Licensee MDPI, Basel, Switzerland. This article is an open access article distributed under the terms and conditions of the Creative Commons Attribution (CC BY) license (<https://creativecommons.org/licenses/by/4.0/>).

Keywords: CCUS; CO₂-EOR and storage; deep learning; lightGBM; transformers

1. Introduction

Due to carbon dioxide greenhouse gas emissions, global warming has become an irreversible trend [1]. In order to mitigate the greenhouse effect, carbon capture, utilization, and storage technology (CCUS) is being widely used [2–4]. Among the different technologies, CO₂-enhanced oil recovery (CO₂-EOR) technology is an effective method that can not only improve oil recovery through CO₂ miscible flooding but can also store CO₂ in oil reservoirs [5,6]. Considering the economic benefits of significantly improving oil recovery and the social benefits of burying carbon and reducing emissions, CO₂-EOR is widely used in oil and gas field development [7]. With the proposal of China's "dual carbon" goals, CO₂-EOR technology has once again ushered in a period of rapid development opportunities [8,9].

The most relevant parameters in CO₂-EOR and storage are oil production, CO₂ storage amount, and Net Present Value (NPV) [10–12]. Among them, oil production and NPV are related to the economic reliability of the project, and CO₂ storage amount is related to whether the goal of effective CO₂ storage can be achieved. Therefore, most studies focus on predicting cumulative oil production, CO₂ storage amount, and NPV. However, due to the high time cost and poor adaptability of experimental methods [13] and traditional numerical methods [14–16], more and more studies tend to use machine learning

methods to establish reliable prediction models for oil recovery and CO₂ storage efficiency. Moosavi et al. tested the ability of hybrid radial basis function (RBF) networks to predict oil recovery and oil rate in CO₂ foam flooding reservoirs [17]. Chen et al. developed an ML model to predict hydrocarbon production potential and CO₂ storage amount in ROZ using multivariate adaptive regression splines (MARSs), support vector machines (SVRs), and random forests (RFs) [18]. You et al. used a multi-layer neural network (MLNN) proxy model to predict cumulative oil production and CO₂ storage amount [19]. However, these models mainly focus on static prediction. They do not provide an overall dynamic prediction, including oil production, CO₂ storage amount, and NPV over time. Some studies have considered dynamic time series prediction. Asante et al. utilized a Long Short-Term Memory (LSTM) neural network to predict the historical oil recovery of oil fields using dynamic data, including pressure, water-alternating-gas (WAG) cycle, and injection volume [20]. Iskandar et al. employed autoregressive (AR), multi-layer perceptron (MLP), and Long Short-Term Memory (LSTM) networks to combine reservoir characteristic parameters and bottom-hole pressure to predict oil, gas, and water production rates [21]. However, these studies usually do not combine static prediction with dynamic prediction, resulting in a lack of comprehensiveness and accuracy in the prediction results. In addition, commonly used data-driven models (such as LSTM) in these studies cannot effectively capture long-term dependencies. Furthermore, their computation times are relatively long, leading to inefficiency. Therefore, an advanced model is needed to efficiently achieve accurate static and dynamic predictions of oil production, CO₂ storage amount, and NPV. This will help to fully understand the oil recovery and CO₂ storage capacity to optimize production plans.

This paper combines a lightweight gradient boosting machine (LightGBM) with Temporal Fusion Transformers and proposes a deep learning framework based on the Light-Trans model to simultaneously realize the dynamic and static prediction of CO₂ flooding and storage capacity. LightGBM is a lightweight machine-learning method with fast speed and high accuracy [22]. So far, it has been widely used in many static prediction tasks in the CCUS industry and has achieved more effective performance than baseline methods [23,24]. In addition, the method based on Temporal Fusion Transformers (TFTs) has shown excellent performance in dynamic time series [25]. TFTs can improve the accuracy of dynamic time series prediction by enhancing static data. More importantly, the method can effectively capture long-term dependencies through a multi-head attention mechanism. It has been widely used and successful in fields such as energy, transportation, and finance [26–28]. Therefore, it is expected to provide reliable real-time predictions for the CCUS field.

We take a typical well group in a low-permeability oil field in Xinjiang as an example to predict CO₂ flooding and storage capacity. With this method, we can not only achieve high-precision static predictions of cumulative oil production, CO₂ storage, and NPV, but we can also make real-time predictions of the dynamic changes in these indicators efficiently, thereby comprehensively evaluating CO₂ flooding and storage capacity.

2. Methodology

2.1. Description of Numerical Models for Field-Scale Oil Reservoirs

The study site was a typical low-permeability oil field in Xinjiang. This oil field has a burial depth ranging from 2158 to 2793 m, geological reserves of 35.23 million metric tons, an average permeability of 6.15 mD, an average porosity of 12.5%, and an average water saturation of 0.58. Based on over 30 years of field data (since 1990) from water injection development, a numerical simulation model for this oil field was established using the 2022 version of CMG-GEM (Computer Modelling Group Ltd., Calgary, AB, Canada). This model has completed history matching and encompasses a wide range of geological and engineering parameters. For the convenience of calculation, we took out a typical well group model of 4 injections and 15 productions that represented the entire oil field from the total numerical model, and the number of model grids was 9000. The schematic diagram of sub-model extraction is shown in Figure 1. The reservoir physical

property parameters are shown in Table 1. The oil–water relative permeability and oil–gas relative permeability curves shown in Figure 2 were obtained through indoor experiments. The crude oil components are shown in Table 2.

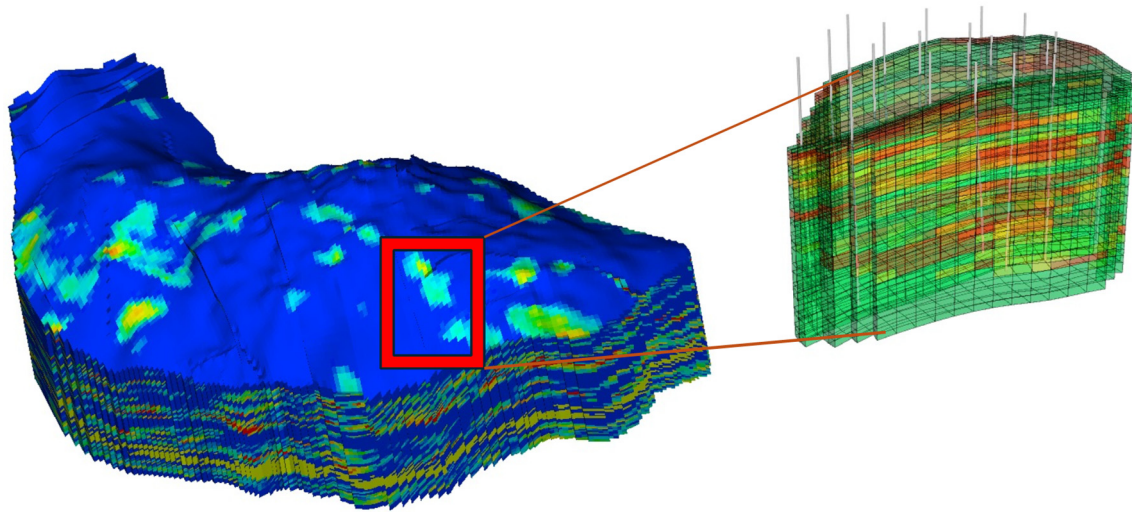


Figure 1. Typical well pattern model extraction from field-scale numerical model.

Table 1. Reservoir properties.

Characteristics	Value
Reservoir temperature/°C	82.6
Geological reserves/million tons	1.69
Original formation pressure/MPa	28.8
Average permeability/mD	6.9
Average porosity/%	12.5
Average water saturation	0.58
Number of grids	9000

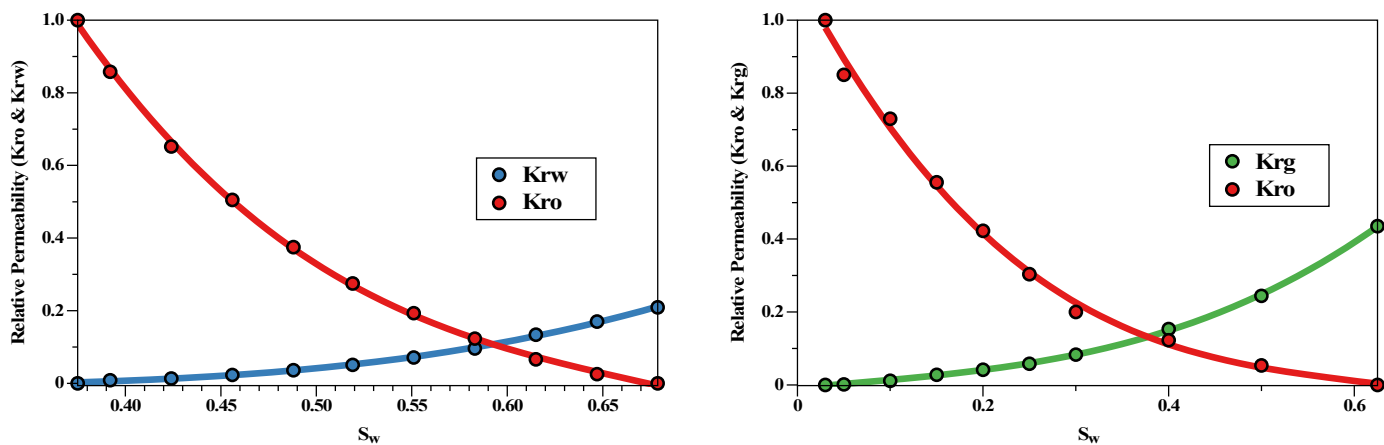


Figure 2. Relative permeability curves of oil–water and oil–gas phases.

Table 2. Composition of crude oil components.

Component	Mole Percentage
CO ₂	0.02
N ₂	1.32
C1	41.57
C2	7.46

Table 2. *Cont.*

Component	Mole Percentage
C3	6.76
iC4	3.72
nC4	3.13
iC5	2.55
nC5	1.45
C6	2.65
C7+	29.3
Sum	100

2.2. Data Preparation

To improve the performance of the intelligent model, we used the Monte Carlo method to perform extensive simulations through 504 parameterized experiments. This method ensures the uniformity of parameter distribution, thereby improving the prediction accuracy of the model. The parameter ranges involved in the Monte Carlo simulation experiments are detailed in Table 3. The input parameters of the model included gas injection time, water injection time, gas injection rate, water injection rate, bottom-hole pressure of the production wells, and maximum liquid production rate. In particular, the bottom-hole pressure and liquid production rate of the production wells were key setting indicators, but they have often been overlooked in previous studies. The bottom-hole pressure is key to controlling miscible flow and pressure difference, while the liquid production rate ensures stable production in low permeability reservoirs with sufficient elastic energy (high gas–oil ratio). The model output included static and dynamic data. The static data cover the cumulative oil production, CO₂ storage, and Net Present Value (NPV) after 20 years of using CO₂ water-alternating-gas (CO₂–WAG) technology. The dynamic data recorded the oil production rate, CO₂ production rate, and time-varying CO₂ storage amount during the 20-year period. To ensure that the model accurately captured these dynamic changes, we extracted up to 438 time series data points from each experiment.

Table 3. Parameter ranges of Monte Carlo simulation experiments (within one WAG cycle).

Parameters	Unit	Min	Max
Gas injection time	day	100	360
Water injection time	day	100	360
Gas injection rate	m ³ /day	80,000	180,000
Water injection rate	m ³ /day	160	360
Bottom hole pressure of production wells	MPa	22	33
Maximum total surface liquid production of production wells	m ³ /day	10	25

2.3. LightTrans Model Framework

LightTrans is a deep learning model that combines LightGBM and Transformers technology, designed specifically for evaluating the CO₂-EOR and storage capacity of oil reservoirs. This model is capable of processing and parsing a large amount of static and dynamic data in oil recovery and storage systems. The LightTrans model framework is shown in Figure 3.

In the LightTrans model, the LightGBM part is responsible for processing and evaluating the static characteristics of the reservoir, such as geological structure and physical properties. The Transformers part processes time series data and predicts the dynamic changes in oil recovery and CO₂ storage by capturing changes in reservoir properties over time. Through this combination, the model not only improves the flexibility of the evaluation but also greatly enhances the accuracy of the prediction.

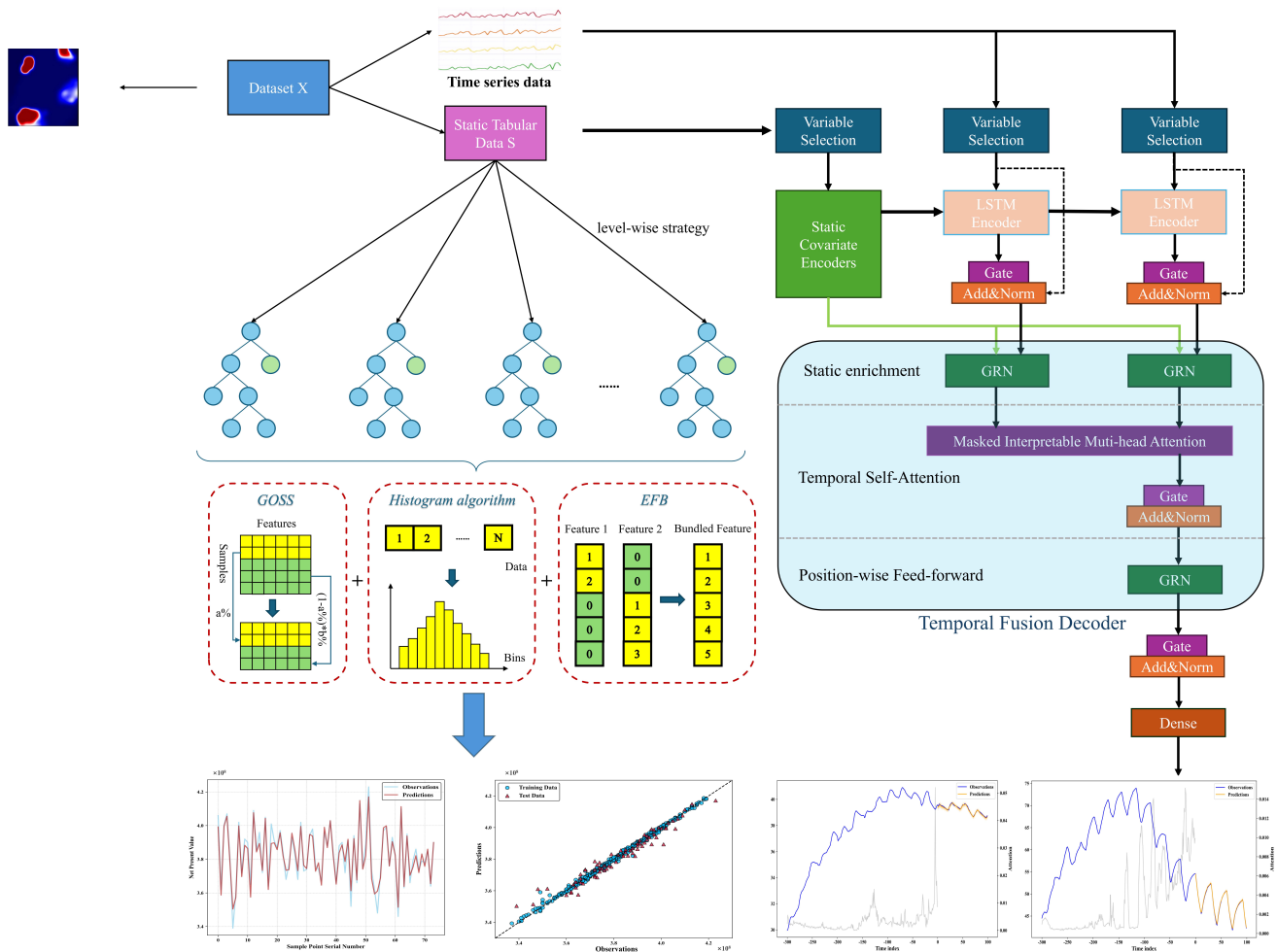


Figure 3. LightTrans model architecture.

LightGBM is an efficient gradient-boosting decision tree algorithm [22,29]. It leverages four key technologies to enhance its performance:

- Gradient-based one-sided sampling (GOSS): Only samples with larger absolute values of gradients are sampled without traversing all samples. Therefore, the amount of calculation is reduced while maintaining the representativeness of the data.
- Histogram-based algorithm: By bucketing continuous feature values into discrete histograms, memory usage is significantly reduced, and time complexity is greatly reduced.
- Exclusive feature bundling (EFB): Bundling mutually exclusive features together reduces the number of processed features and improves the efficiency of the algorithm without reducing accuracy.
- Leaf-wise growth strategy with depth constraints: Compared with the traditional level-wise growth strategy, the leaf-wise strategy pays more attention to areas with higher error rates, effectively reduces the risk of overfitting, and maintains the accuracy of the model.

These unique designs enable LightGBM to process static data efficiently.

For dynamic time series data prediction, Temporal Fusion Transformers (TFTs) outperform all major deep learning models [25]. This is due to their powerful static covariate encoder and temporal multi-head attention mechanism. The static covariate encoder enables the model to make full use of static features and enhance the accuracy of predictions. The temporal self-attention mechanism is used to learn long-term dependencies in time series, which can improve the model’s ability to capture temporal dynamics. This means that TFTs are very suitable for our task. The static covariate encoder uses a separate Gated Residual Network (GRN) encoder to generate four different context vectors for temporal variable

selection, local processing of temporal features, and enrichment of temporal features with static information. Among them, GRN can perform effective nonlinear processing on the input, and its mathematical expression is:

$$\begin{aligned}\text{GRN}_\omega(\mathbf{a}, \mathbf{c}) &= \text{LayerNorm}(\mathbf{a} + \text{GLU}_\omega(\boldsymbol{\eta}_1)) \\ \boldsymbol{\eta}_1 &= \mathbf{W}_{1,\omega}\boldsymbol{\eta}_2 + \mathbf{b}_{1,\omega}, \\ \boldsymbol{\eta}_2 &= \text{ELU}(\mathbf{W}_{2,\omega}\mathbf{a} + \mathbf{W}_{3,\omega}\mathbf{c} + \mathbf{b}_{2,\omega}) \\ \text{GLU}_\omega(\boldsymbol{\gamma}) &= \sigma(\mathbf{W}_{4,\omega}\boldsymbol{\gamma} + \mathbf{b}_{4,\omega}) \odot (\mathbf{W}_{5,\omega}\boldsymbol{\gamma} + \mathbf{b}_{5,\omega})\end{aligned}$$

where LayerNorm represents the Layer Normalization operation. \mathbf{a} is a primary input feature vector. \mathbf{c} is a static variable vector. ELU is the exponential linear unit activation function. GLU stands for Gated Linear Unit. \mathbf{W} and \mathbf{b} are weights and biases. σ is the sigmoid activation function. \odot represents the element-wise multiplication.

The multi-head attention mechanism in TFT is mainly based on the Transformer model of Vaswani et al. [30]. Attention mechanism is a mechanism in neural networks that allows the model to focus on specific parts of the input sequence when making predictions. Its formula is:

$$\text{Attention}(\mathbf{Q}, \mathbf{K}, \mathbf{V}) = \text{softmax}\left(\frac{\mathbf{Q}\mathbf{K}^T}{\sqrt{d_k}}\right)\mathbf{V}$$

where \mathbf{Q} is the query matrix. \mathbf{K} is the key matrix. d_k is the dimension of the key vectors. softmax is the softmax function, which is used to convert the scaled dot products into a probability distribution. \mathbf{V} is the value matrix.

The multi-head attention mechanism is proposed to simultaneously focus on different parts of the input sequence by using multiple attention heads. It is computed as follows:

$$\text{MultiHead}(\mathbf{Q}, \mathbf{K}, \mathbf{V}) = \text{Concat}(\mathbf{H}_1, \mathbf{H}_2, \dots, \mathbf{H}_{m_H})\mathbf{W}^H$$

$$\mathbf{H}_i = \text{Attention}\left(\mathbf{Q}\mathbf{W}_i^Q, \mathbf{K}\mathbf{W}_i^K, \mathbf{V}\mathbf{W}_i^V\right)$$

where \mathbf{W}_i^Q , \mathbf{W}_i^K , and \mathbf{W}_i^V are the weights of each head \mathbf{H}_i , respectively. \mathbf{W}^H is the weight matrix after the output of the multi-head attention mechanism. m_H represents the total number of attention heads. Concat represents the concatenation operation, which combines the outputs of the attention heads into a single matrix.

In addition, in order to emphasize the importance of specific features, an interpretable multi-head attention mechanism is implemented by adding shared value weights. The formula is:

$$\text{InterpretableMultiHead}(\mathbf{Q}, \mathbf{K}, \mathbf{V}) = \tilde{\mathbf{H}}\mathbf{W}_H$$

$$\begin{aligned}\tilde{\mathbf{H}} &= \tilde{\mathbf{A}}(\mathbf{Q}, \mathbf{K})\mathbf{V}\mathbf{W}_V \\ &= \left\{ \frac{1}{H} \sum_{h=1}^{m_H} \mathbf{A}\left(\mathbf{Q}\mathbf{W}_Q^{(h)}, \mathbf{K}\mathbf{W}_K^{(h)}\right) \right\} \mathbf{V}\mathbf{W}_V \\ &= \frac{1}{H} \sum_{h=1}^{m_H} \text{Attention}\left(\mathbf{Q}\mathbf{W}_Q^{(h)}, \mathbf{K}\mathbf{W}_K^{(h)}, \mathbf{V}\mathbf{W}_V\right)\end{aligned}$$

where \mathbf{W}_H is used for the final mapping. $\tilde{\mathbf{H}}$ is the combined output of all attention heads. $\tilde{\mathbf{A}}$ represents the normalized attention scores. \mathbf{W}_V is the value weight shared by all heads. $\mathbf{W}_Q^{(h)}$ and $\mathbf{W}_K^{(h)}$ are the weight matrices for the query and key projections for the h -th head.

In addition, TFTs also utilize Long Short-Term Memory (LSTM) networks as part of their architecture to handle sequential data and capture temporal dependencies.

Overall, our LightTrans model significantly improves the prediction accuracy of engineering static and reservoir dynamic data by combining the efficiency of LightGBM with the powerful time series data processing capabilities of TFTs, especially in oil recovery and CO₂ storage capability. This not only optimizes resource utilization efficiency but also improves the economics of operations.

2.4. Evaluation Indicators

The evaluation indicators of the LightTrans model are set as follows: coefficient of determination R-square (R^2) and mean absolute percentage error (MAPE).

$$\begin{cases} R^2 = 1 - \frac{\sum_i (\hat{y}_i - y_i)^2}{\sum_i (\bar{y}_i - y_i)^2} \\ MAPE = \frac{1}{m} \sum_{i=1}^m \left[\frac{|\hat{y}_i - y_i|}{y_i} \right] \times 100 \end{cases}$$

where \hat{y}_i is the i -th predicted value, y_i is the corresponding observed value, and m is the number of samples.

3. Results and Discussion

3.1. Preliminary Intelligent Evaluation and Model Hyperparameter Adjustment

First, the LightGBM algorithm combining fair-cut trees and the synthetic minority oversampling technique (FCT-SMOTE-LightGBM) model was used to conduct a preliminary evaluation of the CO₂ flooding and storage potential of the typical reservoir blocks in our study. This model has been proven to be applicable to various types of reservoirs. Its description is shown in Figure 4. For details, see our previous publication [31]. The model evaluation result is “good”. Therefore, the low permeability reservoir we studied is suitable for CO₂ flooding. Further, we need to perform dynamic and static predictions of CO₂ flooding and storage capacity for this oil reservoir. The TransLight model was trained using static tabular data from 504 simulation experiments and 220,752 (504 simulation experiments × 438 sampling time series data points) dynamic numerical simulation data to perform static and dynamic predictions of CO₂ flooding and storage capacity. Our deep learning model runs on the PyTorch 2.3 platform using NVIDIA GeForce RTX 4070TI (NVIDIA Corp., Santa Clara, CA, USA).

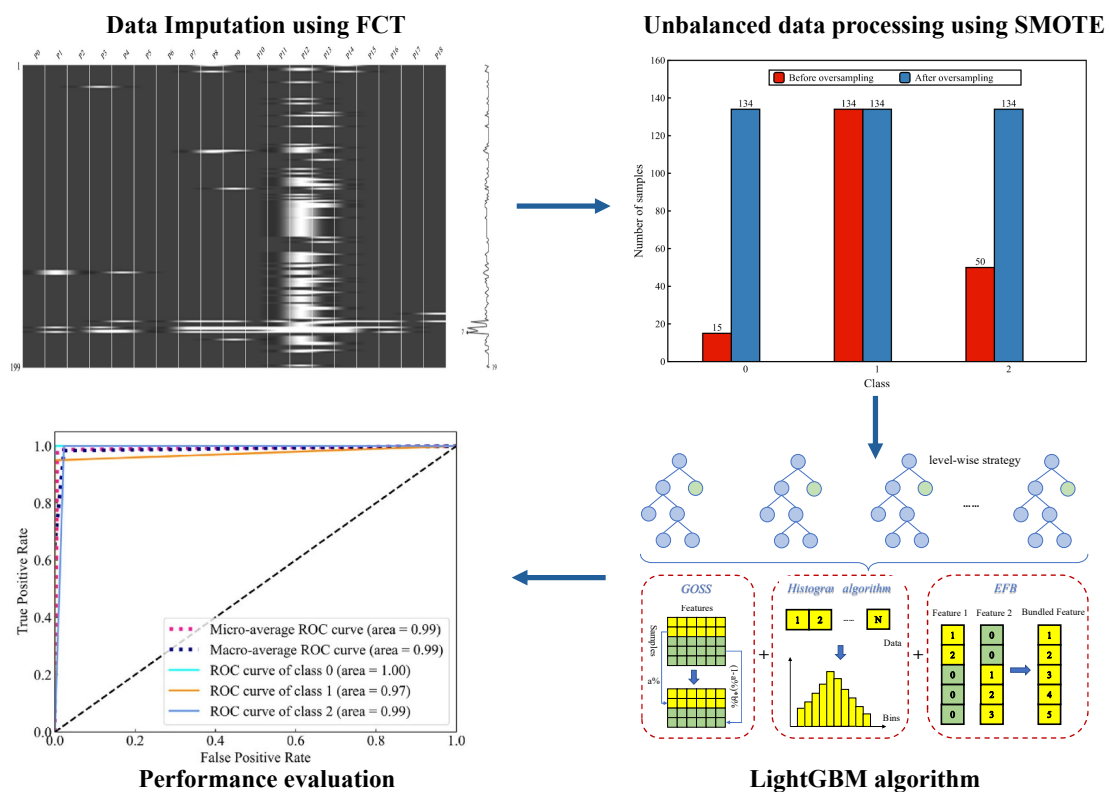


Figure 4. A description of the LightGBM algorithm combining fair-cut trees and the synthetic minority oversampling technique (FCT-SMOTE-LightGBM) model.

3.2. Prediction Performance of TransLight Model

Figure 5 shows the performance of the TransLight model in the static prediction task. It can be observed that the prediction points are almost all located near the 45-degree line, which shows that the model fits very well. Therefore, the TransLight model performs well in the static prediction of cumulative oil production, CO₂ storage amount, and Net Present Value. The specific prediction performance indicators are listed in Table 4. The model has R² values of 0.9426, 0.9616, and 0.9404 and MAPE values of 0.0085, 0.0262, and 0.0081 for cumulative oil production, CO₂ storage amount, and Net Present Value on the test set, respectively. These results show that the TransLight model can provide high-precision predictions on different static targets. The high R² values indicate that the model performs well in explaining data variability, while the low MAPE values indicate that the model has a very small prediction error.

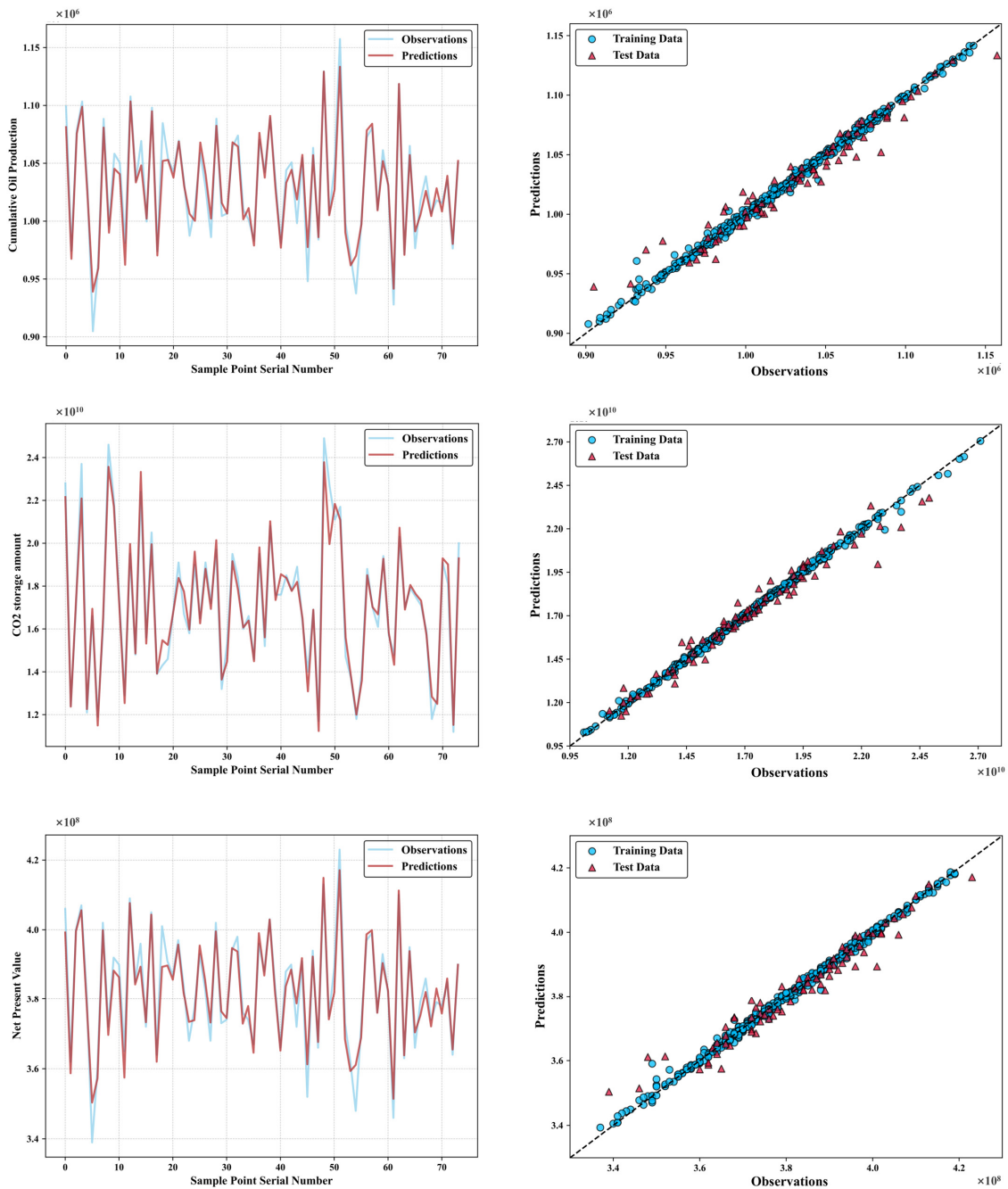


Figure 5. Static prediction performance of the TransLight model.

Table 4. Prediction performance indicators of the TransLight model for three different static targets on training sets and test sets.

Static Targets	Train		Test	
	R ²	MAPE	R ²	MAPE
Cumulative oil production	0.9960	0.0020	0.9426	0.0085
CO ₂ storage amount	0.9982	0.0053	0.9616	0.0262
Net Present Value	0.9957	0.0019	0.9404	0.0081

In summary, the TransLight model shows strong adaptability and accuracy in handling static prediction tasks, and it can provide reliable results in the prediction of cumulative oil production, CO₂ storage amount, and Net Present Value. The efficient performance of this model makes it a powerful tool for research and application in the field of CO₂-EOR.

In order to further verify the rationality of the proposed model, we also analyzed the ranking results of the model for feature importance. The ranking results are shown in Figure 6. We observed that the maximum total surface liquid production rate has the most significant influence on cumulative oil production and Net Present Value, surpassing the importance of most other features by more than one. This is because the constraint on the total surface liquid production naturally controls oil production, thereby influencing the NPV [32]. The gas injection rate has the most significant impact on CO₂ storage amount, with its importance being nearly 2.5 times greater than that of the other features. This is obviously because the gas injection rate directly affects the volume of CO₂ that can be injected and stored in the reservoir [33]. In addition, bottom-hole pressure is crucial to cumulative oil production and NPV because it controls the degree of miscibility and the size of the pressure difference [34]. However, the gas injection time and water injection time have relatively little effect on oil production and NPV but have a greater impact on storage capacity. This reflects the contradiction between oil recovery and storage [19]. Specifically, GAS TIME and WATER TIME greatly influence CO₂ sweep efficiency, thereby affecting the uniformity of CO₂ sequestration [35]. However, in terms of oil production, while GAS TIME and WATER TIME are important for the overall injection process, their direct impact on oil production is limited by more dominant production factors and constraints [36]. The ranking of the factors influencing oil production and NPV is consistent, reflecting that oil production can control NPV better than storage capacity. In addition, the water injection rate does not seem to have much effect on oil production, storage, and NPV. The ranking results are almost consistent with conventional understanding [19,32–36]. This once again proves the effectiveness of the TransLight model.

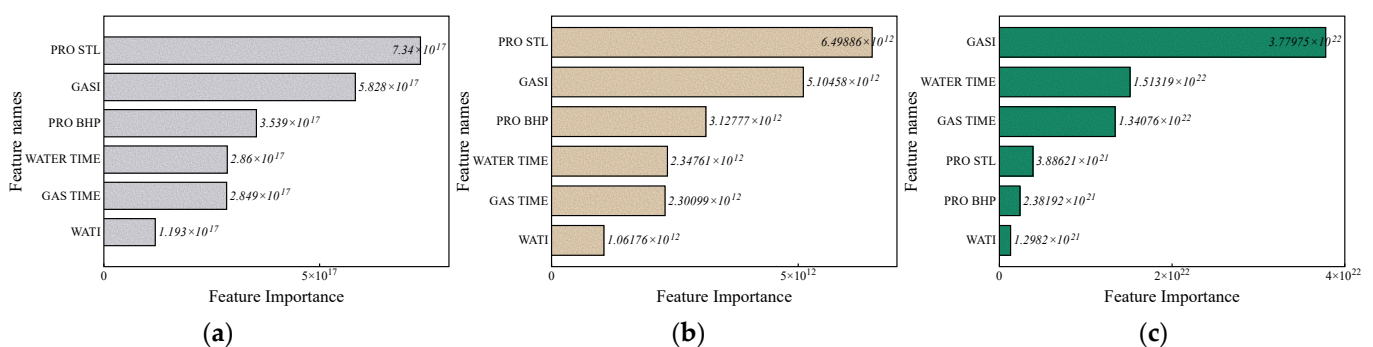


Figure 6. TransLight model shows the feature importance of (a) cumulative oil production, (b) NPV, and (c) CO₂ storage amount, where WATER TIME and GAS TIME represent the water injection time and gas injection time within a cycle, GASI represents the gas injection rate of the injection wells, WATI represents the water injection rate, PRO BHP refers to the bottom-hole pressure of the production wells, and PRO STL indicates the maximum total surface liquid production rate of production wells.

In order to verify the effectiveness of the TransLight model in the dynamic prediction task, we performed a performance evaluation on all samples in the test set. The specific results are shown in Table 5. The proposed model has excellent prediction performance for the three dynamic targets. Specifically, the average R^2 value reaches 0.9998, and the average MAPE value reaches 0.0025. Figures 7–9 show a visual comparison of the TransLight model's predictions and observations for three dynamic targets in four cases that are randomly selected from the Monte Carlo experiment. The parameters of the four cases are shown in Table 6. It can be observed that the TransLight model prediction results are highly consistent with the observed results. In addition, the model successfully captures the volatility of the data. The gray curve represents the attention mechanism. It can be seen that all strong turning points and the places closest to the prediction points receive almost full attention. This proves that the model we proposed performs well in predicting the three dynamic targets of oil production rate, CO_2 production rate, and time-varying CO_2 storage amount, which is highly consistent with expectations. From these results, it can be seen that the TransLight model can not only accurately capture the changing trends of dynamic targets but also provide high-precision prediction results, which further proves the reliability and practicality of the model. We also compared the TransLight model with classic baseline models: AutoRegressive Integrated Moving Average (ARIMA), Long Short-Term Memory (LSTM), and Gated Recurrent Unit (GRU). Table 7 shows the comparison results. We found that the TransLight model achieves the highest average performance in predicting three different dynamic targets. In addition, in terms of computational efficiency, when the data volume is in the range of thousands, the intelligent model is typically 10^4 to 10^6 times faster than traditional numerical simulation methods [37,38]. It is worth noting that the computation speed of our intelligent model is 3–20 s. However, the running time of 504 numerical experiments is nearly 504 h (nearly 1,814,400 s). This means that our model is nearly 10^5 – 10^6 times faster than traditional numerical simulation methods. The superior performance of this model provides an efficient and accurate solution for the dynamic prediction of CO_2 flooding and storage capacity.

Table 5. Prediction performance indicators of TransLight model for three different dynamic targets on test sets.

Dynamic Targets	R^2	MAPE
Oil production rate	0.9998	0.0016
CO_2 production rate	0.9997	0.0047
Time-varying CO_2 storage amount	0.9998	0.0012
Average	0.9998	0.0025

Table 6. Parameter presentation of four random cases selected from the Monte Carlo simulation experiment.

	GASI (m^3/day)	WATI (m^3/day)	GAS TIME (day)	WATER TIME (day)	PRO BHP (MPa)	PRO STL (m^3/day)
Case 1	115,108.04	311.63	128.18	254.38	24.14	15.63
Case 2	119,860.58	285.90	216.38	299.69	23.04	15.67
Case 3	133,017.68	236.13	297.72	162.79	27.75	17.93
Case 4	150,117.93	312.88	291.12	224.79	25.20	20.78

Table 7. Average performance comparison of TransLight model and baseline models for three different dynamic targets on test sets (* indicates a very small value, meaning the performance is poor).

Model	R^2	MAPE
ARIMA	*	0.3329
LSTM	0.9606	0.0465
GRU	0.9795	0.0258
TransLight	0.9998	0.0025

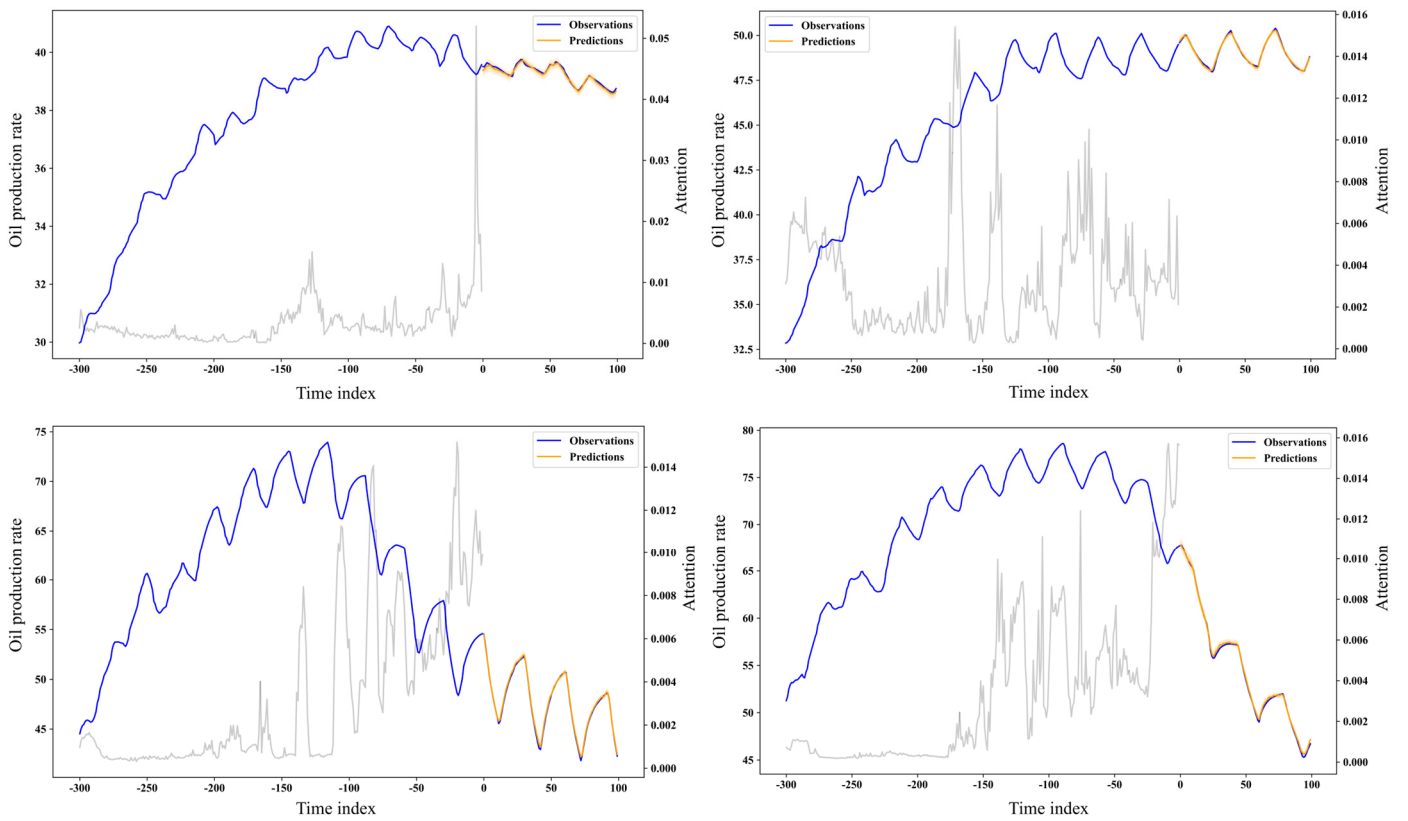


Figure 7. Dynamic prediction curve of oil production rate by TransLight model (four cases are shown).

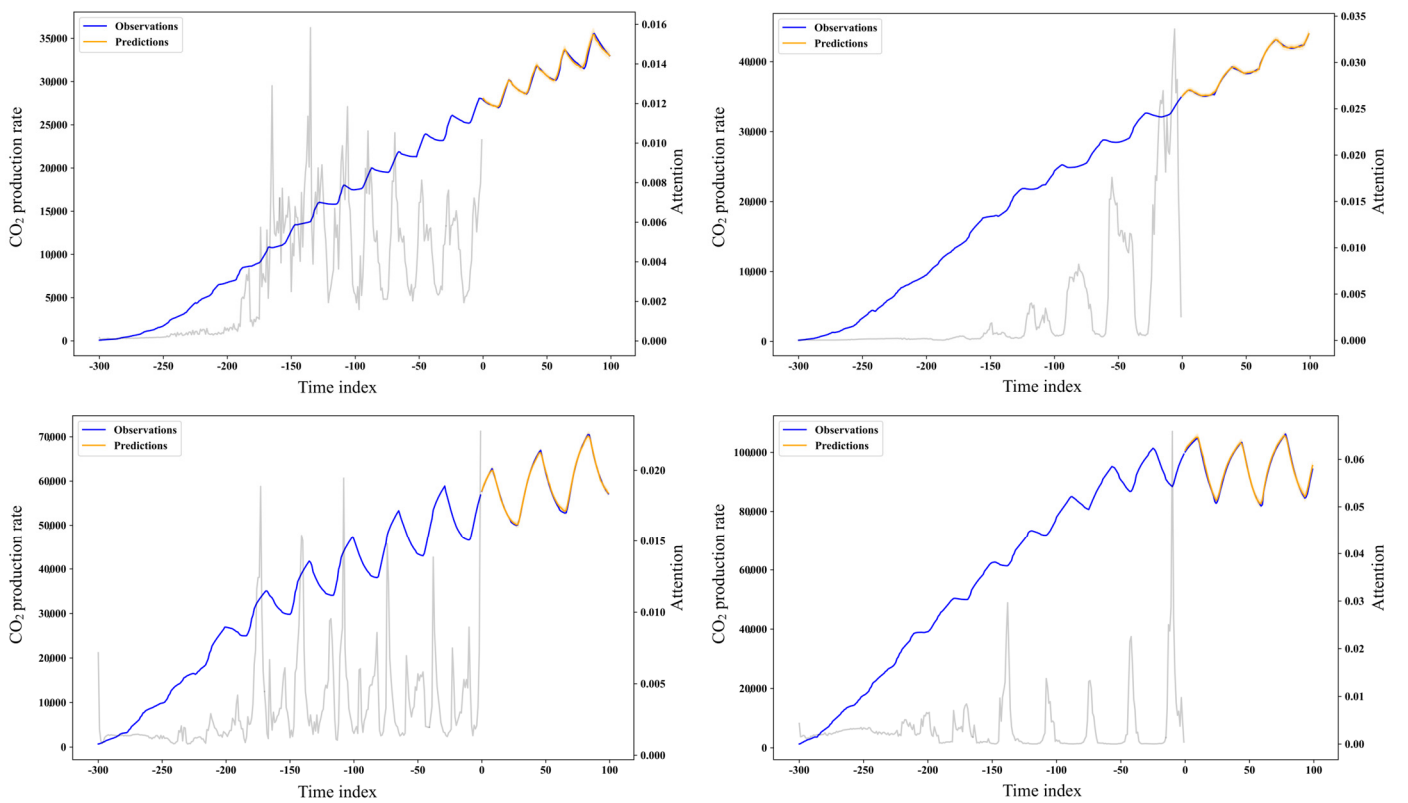


Figure 8. Dynamic prediction curve of CO₂ production rate by TransLight model (four cases are shown).

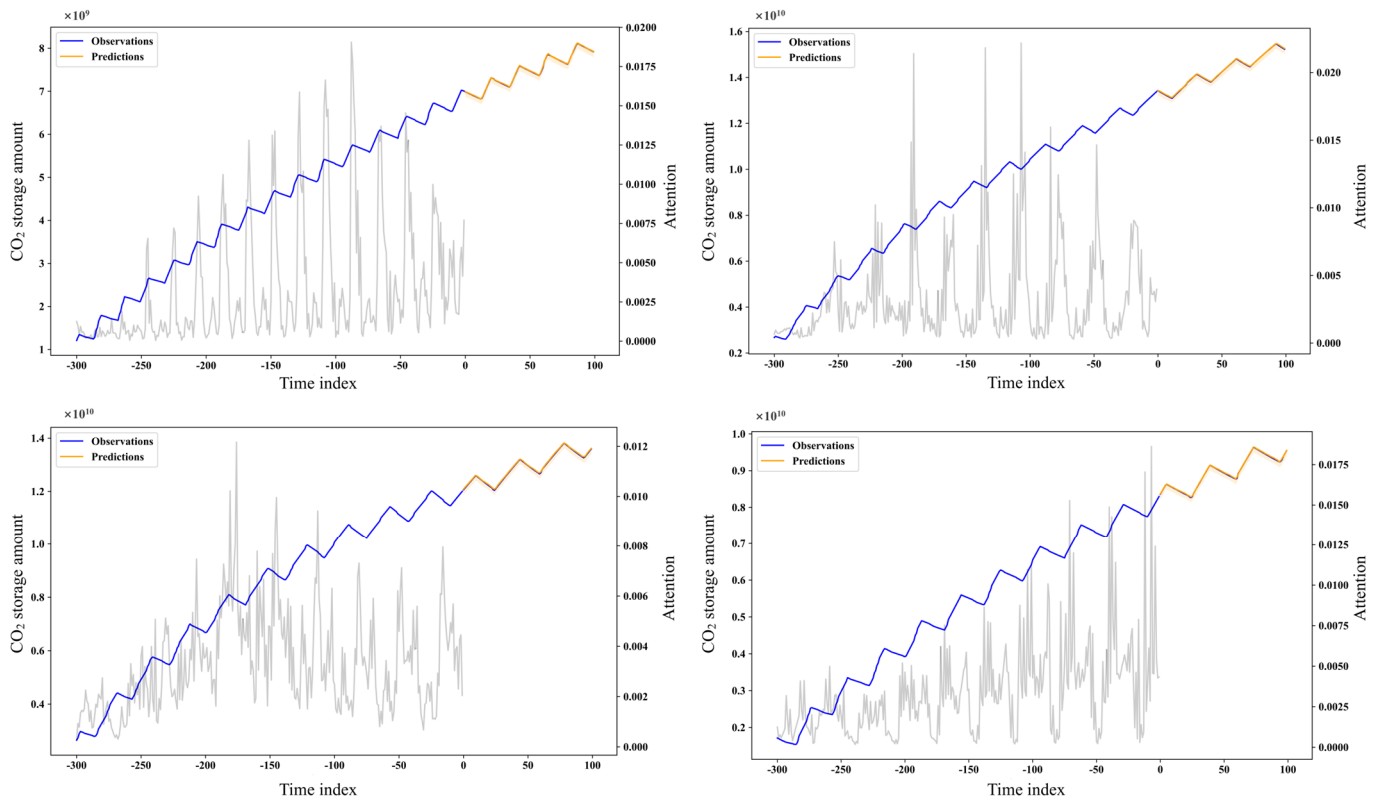


Figure 9. Dynamic prediction of time-varying CO₂ storage amount by TransLight model (four cases are shown).

4. Conclusions

In this study, we propose a deep learning framework based on the LightTrans model to perform dynamic and static modeling of CO₂ flooding storage capabilities. We show that the LightTrans model can achieve high-precision dynamic and static predictions in CO₂ flooding storage prediction tasks. The average R² for static forecasts is 0.9482, and the mean absolute percentage error (MAPE) is 0.0143. The average R² of dynamic prediction is 0.9998, and MAPE is 0.0025. The LightTrans model successfully predicted cumulative oil production, CO₂ storage capacity, NPV, and the time-varying capacity of the oil displacement and storage system in real time. The model not only accurately captures the volatility and important trends of these variables but also significantly improves forecast efficiency. Our model is 10⁵ to 10⁶ times faster in calculation speed than traditional numerical simulation. In addition, because the LightTrans model can predict oil displacement and storage information under different scenarios, it can be used as an efficient alternative to numerical simulation. In the future, the LightTrans model can also be used to optimize injection and production plans and make probabilistic predictions of important dynamic information, such as pressure changes, further improving the efficiency of oil field management and CO₂ storage. Through these results, it can be seen that the LightTrans model has significant potential for application in the field of CO₂ oil displacement and storage. It can not only improve the accuracy of prediction but also significantly shorten the calculation time, providing an efficient and effective method for oil field development and management.

Although our model has the advantages of high accuracy and efficiency, its shortcomings in terms of high data requirements, tuning complexity, and interpretability still need to be balanced and optimized in practical applications.

Author Contributions: Conceptualization, B.S.; methodology, B.S. and K.Y.; validation, S.Y. and J.Y.; formal analysis, Y.Z. and K.Y.; investigation, Y.Z.; resources, Z.X. and J.Y.; data curation, Z.X. and J.Y.; writing—original draft preparation, Z.X. and B.S.; writing—review and editing, Z.X., B.S. and S.Y.; visualization, B.S.; supervision, B.S. and S.Y.; project administration, Z.X. and S.Y.; funding acquisition, Z.X. and S.Y. All authors have read and agreed to the published version of the manuscript.

Funding: This research is supported by PetroChina’s major science and technology projects (No. 2017E-0407).

Data Availability Statement: The data that have been used are confidential.

Conflicts of Interest: Authors Zhipeng Xiao, Jiguang Yang and Yanbin Zhang were employed by the Exploration and Development Research Institute, PetroChina Tuha Oil & Gasfield Company. The remaining authors declare that the research was conducted in the absence of any commercial or financial relationships that could be construed as a potential conflict of interest. The Exploration and Development Research Institute, PetroChina Tuha Oil & Gasfield Company had no role in the design of the study; in the collection, analyses, or interpretation of data; in the writing of the manuscript, or in the decision to publish the results.

References

- Solomon, S.; Plattner, G.-K.; Knutti, R.; Friedlingstein, P. Irreversible Climate Change Due to Carbon Dioxide Emissions. *Proc. Natl. Acad. Sci. USA* **2009**, *106*, 1704–1709. [[CrossRef](#)] [[PubMed](#)]
- Zhang, Z.; Pan, S.-Y.; Li, H.; Cai, J.; Olabi, A.G.; Anthony, E.J.; Manovic, V. Recent Advances in Carbon Dioxide Utilization. *Renew. Sustain. Energy Rev.* **2020**, *125*, 109799. [[CrossRef](#)]
- Yan, Y.; Borhani, T.N.; Subraveti, S.G.; Pai, K.N.; Prasad, V.; Rajendran, A.; Nkulikiyinka, P.; Asibor, J.O.; Zhang, Z.; Shao, D.; et al. Harnessing the Power of Machine Learning for Carbon Capture, Utilisation, and Storage (CCUS)—A State-of-the-Art Review. *Energy Environ. Sci.* **2021**, *14*, 6122–6157. [[CrossRef](#)]
- Gao, X.; Yang, S.; Tian, L.; Shen, B.; Bi, L.; Zhang, Y.; Wang, M.; Rui, Z. System and Multi-Physics Coupling Model of Liquid-CO₂ Injection on CO₂ Storage with Enhanced Gas Recovery (CSEGR) Framework. *Energy* **2024**, *294*, 130951. [[CrossRef](#)]
- Dou, L.; Sun, L.; Lyu, W.; Wang, M.; Gao, F.; Gao, M.; Jiang, H. Trend of Global Carbon Dioxide Capture, Utilization and Storage Industry and Challenges and Countermeasures in China. *Pet. Explor. Dev.* **2023**, *50*, 1246–1260. [[CrossRef](#)]
- Sun, Q.; Ampomah, W.; Kutsienyo, E.J.; Appold, M.; Adu-Gyamfi, B.; Dai, Z.; Soltanian, M.R. Assessment of CO₂ Trapping Mechanisms in Partially Depleted Oil-Bearing Sands. *Fuel* **2020**, *278*, 118356. [[CrossRef](#)]
- Ampomah, W.; Balch, R.S.; Cather, M.; Will, R.; Gonda, D.; Dai, Z.; Soltanian, M.R. Optimum Design of CO₂ Storage and Oil Recovery under Geological Uncertainty. *Appl. Energy* **2017**, *195*, 80–92. [[CrossRef](#)]
- Yuan, S.; Ma, D.; Li, J.; Zhou, T.; Ji, Z.; Han, H. Progress and Prospects of Carbon Dioxide Capture, EOR-Utilization and Storage Industrialization. *Pet. Explor. Dev.* **2022**, *49*, 955–962. [[CrossRef](#)]
- Song, X.; Wang, F.; Ma, D.; Gao, M.; Zhang, Y. Progress and prospect of carbon dioxide capture, utilization and storage in CNPC oilfields. *Pet. Explor. Dev.* **2023**, *50*, 229–244. [[CrossRef](#)]
- Thanh, H.V.; Sugai, Y.; Sasaki, K. Application of Artificial Neural Network for Predicting the Performance of CO₂ Enhanced Oil Recovery and Storage in Residual Oil Zones. *Sci. Rep.* **2020**, *10*, 18204. [[CrossRef](#)]
- You, J.; Ampomah, W.; Sun, Q.; Kutsienyo, E.J.; Balch, R.S.; Dai, Z.; Cather, M.; Zhang, X. Machine Learning Based Co-Optimization of Carbon Dioxide Sequestration and Oil Recovery in CO₂-EOR Project. *J. Clean. Prod.* **2020**, *260*, 120866. [[CrossRef](#)]
- Ren, B.; Male, F.; Duncan, I.J. Economic Analysis of CCUS: Accelerated Development for CO₂ EOR and Storage in Residual Oil Zones under the Context of 45Q Tax Credit. *Appl. Energy* **2022**, *321*, 119393. [[CrossRef](#)]
- Chen, H.; Liu, X.; Zhang, C.; Tan, X.; Yang, R.; Yang, S.; Yang, J. Effects of Miscible Degree and Pore Scale on Seepage Characteristics of Unconventional Reservoirs Fluids Due to Supercritical CO₂ Injection. *Energy* **2022**, *239*, 122287. [[CrossRef](#)]
- Gao, X.; Yang, S.; Shen, B.; Tian, L.; Li, S.; Zhang, X.; Wang, J. Influence of Reservoir Spatial Heterogeneity on a Multicoupling Process of CO₂ Geological Storage. *Energy Fuels* **2023**, *37*, 14991–15005. [[CrossRef](#)]
- Li, Z.; Su, Y.; Li, L.; Hao, Y.; Wang, W.; Meng, Y.; Zhao, A. Evaluation of CO₂ Storage of Water Alternating Gas Flooding Using Experimental and Numerical Simulation Methods. *Fuel* **2022**, *311*, 122489. [[CrossRef](#)]
- Hu, J.; Yang, S.; Yang, K.; Deng, H.; Wang, M.; Li, J.; Gao, X. Enhanced Gas Recovery Coupled with CO₂ Sequestration in Tight Sandstone Reservoirs with Different Pore-Throat Structures. *Energy Fuels* **2024**, *38*, 12005–12023. [[CrossRef](#)]
- Moosavi, S.R.; Wood, D.A.; Samadani, S.A. Modeling Performance of Foam-CO₂ Reservoir Flooding with Hybrid Machine-Learning Models Combining a Radial Basis Function and Evolutionary Algorithms. *Comput. Res. Prog. Appl. Sci. Eng.* **2020**, *6*, 1–8.
- Chen, B.; Pawar, R.J. Characterization of CO₂ Storage and Enhanced Oil Recovery in Residual Oil Zones. *Energy* **2019**, *183*, 291–304. [[CrossRef](#)]
- You, J.; Ampomah, W.; Sun, Q. Co-Optimizing Water-Alternating-Carbon Dioxide Injection Projects Using a Machine Learning Assisted Computational Framework. *Appl. Energy* **2020**, *279*, 115695. [[CrossRef](#)]

20. Asante, J.; Ampomah, W.; Tu, J.; Cather, M. Data-Driven Modeling for Forecasting Oil Recovery: A Timeseries Neural Network Approach for Tertiary CO₂ WAG EOR. *Geoenergy Sci. Eng.* **2024**, *233*, 212555. [[CrossRef](#)]
21. Iskandar, U.P.; Kurihara, M. Time-Series Forecasting of a CO₂-EOR and CO₂ Storage Project Using a Data-Driven Approach. *Energies* **2022**, *15*, 4768. [[CrossRef](#)]
22. Ke, G.; Meng, Q.; Finley, T.; Wang, T.; Chen, W.; Ma, W.; Ye, Q.; Liu, T.-Y. LightGBM: A Highly Efficient Gradient Boosting Decision Tree. In Proceedings of the Advances in Neural Information Processing Systems, Long Beach, CA, USA, 4–9 December 2017; Volume 30.
23. Huang, Z.; Chen, Z. Comparison of Different Machine Learning Algorithms for Predicting the SAGD Production Performance. *J. Pet. Sci. Eng.* **2021**, *202*, 108559. [[CrossRef](#)]
24. Shen, B.; Yang, S.; Hu, J.; Gao, Y.; Xu, H.; Gao, X.; Chen, H. Application of Heterogeneous Ensemble Learning for CO₂—Brine Interfacial Tension Prediction: Implications for CO₂ Storage. *Energy Fuels* **2024**, *38*, 4401–4416. [[CrossRef](#)]
25. Lim, B.; Arik, S.O.; Loeff, N.; Pfister, T. Temporal Fusion Transformers for Interpretable Multi-Horizon Time Series Forecasting. *Int. J. Forecast.* **2021**, *37*, 1748–1764. [[CrossRef](#)]
26. Wu, B.; Wang, L.; Zeng, Y.-R. Interpretable Wind Speed Prediction with Multivariate Time Series and Temporal Fusion Transformers. *Energy* **2022**, *252*, 123990. [[CrossRef](#)]
27. Zhang, H.; Zou, Y.; Yang, X.; Yang, H. A Temporal Fusion Transformer for Short-Term Freeway Traffic Speed Multistep Prediction. *Neurocomputing* **2022**, *500*, 329–340. [[CrossRef](#)]
28. Hu, X. Stock Price Prediction Based on Temporal Fusion Transformer. In Proceedings of the 2021 3rd International Conference on Machine Learning, Big Data and Business Intelligence (MLBDBI), Taiyuan, China, 3–5 December 2021; pp. 60–66.
29. Sheng, K.; Jiang, G.; Du, M.; He, Y.; Dong, T.; Yang, L. Interpretable Knowledge-Guided Framework for Modeling Reservoir Water-Sensitivity Damage Based on Light Gradient Boosting Machine Using Bayesian Optimization and Hybrid Feature Mining. *Eng. Appl. Artif. Intell.* **2024**, *133*, 108511. [[CrossRef](#)]
30. Vaswani, A.; Shazeer, N.; Parmar, N.; Uszkoreit, J.; Jones, L.; Gomez, A.N.; Kaiser, L.; Polosukhin, I. Attention Is All You Need. *arXiv* **2023**, arXiv:1706.03762.
31. Shen, B.; Yang, S.; Gao, X.; Li, S.; Ren, S.; Chen, H. A Novel CO₂-EOR Potential Evaluation Method Based on BO-LightGBM Algorithms Using Hybrid Feature Mining. *Geoenergy Sci. Eng.* **2023**, *222*, 211427. [[CrossRef](#)]
32. Ettehadtavakkol, A.; Lake, L.W.; Bryant, S.L. CO₂-EOR and Storage Design Optimization. *Int. J. Greenh. Gas Control* **2014**, *25*, 79–92. [[CrossRef](#)]
33. Li, H.; Gong, C.; Liu, S.; Xu, J.; Imani, G. Machine Learning-Assisted Prediction of Oil Production and CO₂ Storage Effect in CO₂-Water-Alternating-Gas Injection (CO₂-WAG). *Appl. Sci.* **2022**, *12*, 10958. [[CrossRef](#)]
34. Feng, H.; Haidong, H.; Yanqing, W.; Jianfeng, R.; Liang, Z.; Bo, R.; Butt, H.; Shaoran, R.; Guoli, C. Assessment of Miscibility Effect for CO₂ Flooding EOR in a Low Permeability Reservoir. *J. Pet. Sci. Eng.* **2016**, *145*, 328–335. [[CrossRef](#)]
35. Jia, B.; Tsau, J.-S.; Barati, R. A Review of the Current Progress of CO₂ Injection EOR and Carbon Storage in Shale Oil Reservoirs. *Fuel* **2019**, *236*, 404–427. [[CrossRef](#)]
36. Izadmehr, M.; Daryasafar, A.; Bakhshi, P.; Tavakoli, R.; Ghayyem, M.A. Determining Influence of Different Factors on Production Optimization by Developing Production Scenarios. *J. Pet. Explor. Prod. Technol.* **2018**, *8*, 505–520. [[CrossRef](#)]
37. Wen, G.; Li, Z.; Long, Q.; Azzadenesheli, K.; Anandkumar, A.; Benson, S.M. Real-Time High-Resolution CO₂ Geological Storage Prediction Using Nested Fourier Neural Operators. *Energy Environ. Sci.* **2023**, *16*, 1732–1741. [[CrossRef](#)]
38. Wen, G.; Hay, C.; Benson, S.M. CCSNet: A Deep Learning Modeling Suite for CO₂ Storage. *Adv. Water Resour.* **2021**, *155*, 104009. [[CrossRef](#)]

Disclaimer/Publisher’s Note: The statements, opinions and data contained in all publications are solely those of the individual author(s) and contributor(s) and not of MDPI and/or the editor(s). MDPI and/or the editor(s) disclaim responsibility for any injury to people or property resulting from any ideas, methods, instructions or products referred to in the content.